Research Paper

PAIN®

OPEN

Long-term neuropathic pain behaviors correlate with synaptic plasticity and limbic circuit alteration: a comparative observational study in mice

Francesca Guida[a,*], Monica Iannotta[a], Gabriella Misso[b], Flavia Ricciardi[a], Serena Boccella[a], Virginia Tirino[a], Michela Falco[b], Vincenzo Desiderio[a], Rosmara Infantino[a], Gorizio Pieretti[c], Vito de Novellis[a], Gianpaolo Papaccio[a], Livio Luongo[a,d], Michele Caraglia[b], Sabatino Maione[a,d]

Abstract

Neuropathic pain has long-term consequences in affective and cognitive disturbances, suggesting the involvement of supraspinal mechanisms. In this study, we used the spared nerve injury (SNI) model to characterize the development of sensory and aversive components of neuropathic pain and to determine their electrophysiological impact across prefrontal cortex and limbic regions. Moreover, we evaluated the regulation of several genes involved in immune response and inflammation triggered by SNI. We showed that SNI led to sensorial hypersensitivity (cold and mechanical stimuli) and depressive-like behavior lasting 12 months after nerve injury. Of interest, changes in nonemotional cognitive tasks (novel object recognition and Y maze) showed in 1-month SNI mice were not evident normal in the 12-month SNI animals. In vivo electrophysiology revealed an impaired long-term potentiation at prefrontal cortex-nucleus accumbens core pathway in both the 1-month and 12-month SNI mice. On the other hand, a reduced neural activity was recorded in the lateral entorhinal cortex-dentate gyrus pathway in the 1-month SNI mice, but not in the 12-month SNI mice. Finally, we observed the upregulation of specific genes involved in immune response in the hippocampus of 1-month SNI mice, but not in the 12-month SNI mice, suggesting a neuroinflammatory response that may contribute to the SNI phenotype. These data suggest that distinct brain circuits may drive the psychiatric components of neuropathic pain and pave the way for better investigation of the long-term consequences of peripheral nerve injury for which most of the available drugs are to date unsatisfactory.

Keywords: Spared nerve injury, Neuropathic pain, Behavior, Electrophysiology, Immune system

1. Introduction

Pain chronicization causes cellular reorganization and functional changes in brain regions controlling affective behavior and cognition. Indeed, besides sensorial dysfunctions, patients with chronic or neuropathic pain may refer emotional problems, including depression, and poor performance in learning and memory.[26] Although these comorbidities are clinically recognized, the underlying mechanisms remained unclear. The occurrence of plastic changes in corticolimbic structures (ie, prefrontal cortex, amygdala, hippocampus, and nucleus accumbens) has been indicated as the consequence of the emotional association with the painful stimulus.[48,54] This neural plasticity ranges from functional to structural changes in neurons and may serve as biomarkers for neuropathic pain. Neuroinflammation and immune mechanisms are included among the factors that have been implicated in pain pathophysiology.[2,11,20,47] In the brain, increased levels of proinflammatory molecules released by resident immune cells can participate in the maladaptive neural reorganization and contribute to both sensorial and affective components of neuropathic pain.[32,45]

In this study, we used a multidisciplinary approach to characterize the affective and cognitive consequences of long-term neuropathic pain. To perform this, we adopted the spared nerve injury (SNI) model that reproduces the abnormal pain and related comorbidities by mimicking human experience.[34] Pain together with depressive-like behaviors and cognitive performances has been evaluated 12 months after SNI.

To investigate possible brain functional alterations accompanying behavioral changes, we evaluated synaptic plasticity (long-term potentiation [LTP]) at prefrontal cortex (PFC)-nucleus accumbens core (NAcore) and at lateral entorhinal cortex (LEC)-dentate gyrus (DG) levels. These pathways represent key circuits controlling affective behaviors and reward, which have been recently shown to play a role in chronic pain development.[10,68] Moreover, we have evaluated the contribution of

Sponsorships or competing interests that may be relevant to content are disclosed at the end of this article.

Departments of [a] Experimental Medicine, [b] Precision Medicine, and, [c] Plastic Surgery, University of Campania "Luigi Vanvitelli", Naples, Italy, [d] IRCSS, Neuromed, Neuropharmacology Division, Pozzilli, Italy

**Corresponding author. Address: Department of Experimental Medicine, University of Campania "L. Vanvitelli", 80138 Naples, Italy. Tel.: +39-0815667658. E-mail address: franc.guida@gmail.com (F. Guida).*

Supplemental digital content is available for this article. Direct URL citations appear in the printed text and are provided in the HTML and PDF versions of this article on the journal's Web site (www.painjournalonline.com).

PAIN 163 (2022) 1590–1602

Copyright © 2021 The Author(s). Published by Wolters Kluwer Health, Inc. on behalf of the International Association for the Study of Pain. This is an open access article distributed under the terms of the Creative Commons Attribution-Non Commercial-No Derivatives License 4.0 (CCBY-NC-ND), where it is permissible to download and share the work provided it is properly cited. The work cannot be changed in any way or used commercially without permission from the journal.

http://dx.doi.org/10.1097/j.pain.0000000000002549

immune system through (1) the analysis of PFC and hippocampal gene expression of immune players in neuroinflammation and (2) the analysis of the percentage of specialized subpopulation of regulatory T cells (Tregs) with immunosuppressive properties in neuropathic animals.

To the best of our knowledge, this study is the first showing the behavioral and electrophysiological characterization of a model of peripheral neuropathy for a long time. Our data suggest a possible correlation between specific behavioral deficits of SNI and brain circuit dysfunctions across PFC and limbic region. Moreover, we provide a resource of the changes in immune-related gene expression induced by long-term neuropathic pain in 2 distinct brain regions, which may suggest new molecular pathways in neuropathic pain.

2. Methods

2.1. Animals

Eight-week-old male C57BL/6J mice (Harlan, Italy) were housed 3 per cage under controlled illumination (12 hours light/dark cycle; light on at 6:00 AM) and standard environmental conditions (ambient temperature 20-22°C, humidity 55%-60%). Mice chow and tap water were available ad libitum. The experimental procedures were approved by the Animal Ethics Committee of University of Campania "L. Vanvitelli," Naples. Animal care followed Italian (D.L. 116/92) and European Commission (O.J. of E.C. L358/1 18/12/86) regulations on the protection of laboratory animals. All efforts were made to reduce both animal numbers and distress during the experiments. After 1 week of acclimation, animals were submitted to neuropathic pain induction. Behavioral tasks were performed at different time points (1 and 12 months) in separated groups of animals. The testing was scheduled to avoid carryover effects from previous testing experience. Next, animals were subjected to biochemical evaluations. A separate group of animals was used for in vivo electrophysiological recording. A simplified scheme of behavioral, biochemical, and electrophysiological characterization of sham and SNI animals is given in **Figure 1A**.

2.2. Neuropathy induction

2.2.1. The spared nerve injury

Mononeuropathy was induced according to the method of Decosterd and Woolf.[23] Mice were anesthetized by an intraperitoneal injection of tribromoethanol (250 mg/kg). The sciatic nerve (right side) was exposed at the level of its trifurcation into sural, tibial, and common peroneal nerves. The tibial and common peroneal nerves were ligated tightly with 7.0-silk threads and then transected just distal to the ligation, leaving the sural nerve intact. In sham mice, the sciatic nerve was exposed, but it was not transected.

2.3. Nociceptive behavior

2.3.1. Tactile allodynia

Tactile allodynia was evaluated at a series of calibrated nylon von Frey monofilaments (Ugo Basile, Varese, Italy). Mice were allowed in the compartment of the enclosure positioned on the metal mesh surface. Mice were adapted to the testing environment for 30 minutes before any measurement was taken. The monofilaments, starting from the 0.008 g monofilament, were applied perpendicularly to the plantar surface of each hind paw until it bends in a series of ascending forces (0.008, 0.02, 0.04, 0.07, 0.16, 0.40, 0.60, 1.0, 1.4, and 2.0 g). Each stimulus was applied for approximately 1 second with an interstimulus interval of 5 seconds. Withdrawal responses evoked by each monofilament was obtained from 3 consecutive trials. The mean of paw withdrawal thresholds (PWTs) expressed in grams was reported for each experimental group. A positive response is quick paw withdrawal, licking, or shaking of the paw during application of the monofilament or immediately after the removal of the filament. Voluntary movement, associated with the locomotion, was not counted as a withdrawal response. Tactile allodynia was defined as a significant decrease in the withdrawal threshold to the von Frey hair application. Each mouse served as its own control, the responses being measured both before and after surgical procedure.[9]

2.3.2. Acetone evaporation test

In the acetone evaporation test, cold allodynia and the aversive behaviors elicited by evaporative cooling were measured, adopted by Deuis et al.[25] Acetone was applied on the plantar surface of the hind paw. During cold allodynia assessment in the hind paw, acetone was applied alternately 3 times to each paw, and the response to acetone test was scored by the severity of the response (0: no response, 1: quick withdrawal or flick of the paw, 2: prolonged withdrawal or repeated flicking of the paw, 3: repeated flicking of the hind paw and licking of the paw and the number or duration of nocifensive responses can also be quantified). The test was repeated 5 times with 5-minute intervals, starting from the contralateral side, and a positive response was expressed as withdrawal latency.

2.4. Depressive-like behavior

2.4.1. Tail suspension test

In the tail suspension test, mice were individually suspended by the tail on a horizontal bar (55 cm from floor) using adhesive tape placed approximately 4 cm from the tip of the tail. The duration of immobility, recorded in seconds, was monitored during the last 4 minutes of the 6-minute test by a time recorder. Immobility time was defined as the absence of escape-oriented behavior. Mice were considered to be immobile when they did not show any body movement, hung passively and completely motionless.[33]

2.4.2. Splash test

The splash test, described by Yalcin et al.,[67] consists of spraying a 10% sucrose solution on the back of mice in their home cage. Because of its viscosity, the sucrose solution dirties the coat and induces grooming behavior. Duration of grooming(s) over a 5-minute period was recorded in our experiments.

2.5. Cognitive performances

2.5.1. Novel object recognition test

To assess learning and long-term memory, the novel object recognition (NOR) task was used. Two identical objects were placed into the arena during a 6-minute sample phase. One of the objects was exchanged by a new object, and memory was assessed by comparing the time spent exploring the novel object when compared with the time spent exploring the familiar object during a 5-minute test phase. Two weeks before the NOR experiments, the animals experienced handling by the experimenter

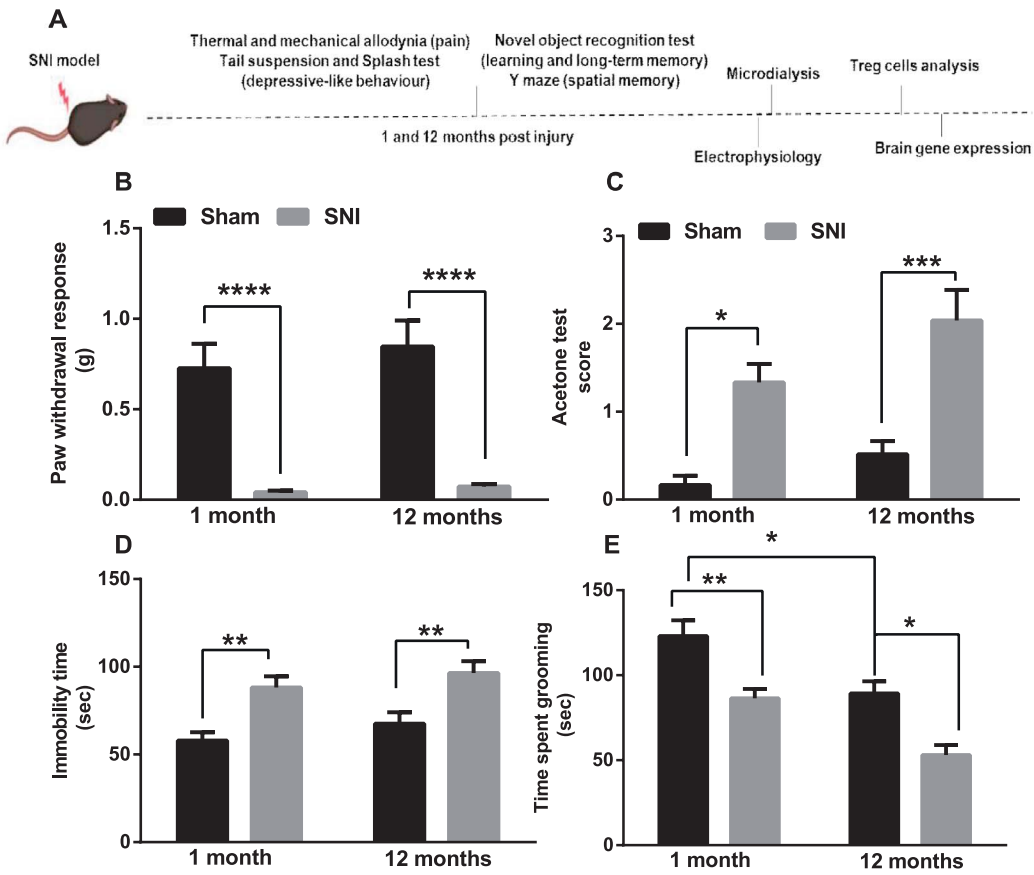

Figure 1. Effects of short-lasting and long-lasting SNI on pain and depressive-like behaviors. (B) Shows paw withdrawal thresholds (PWTs) measured through von Frey monofilaments; (C) shows the score in the acetone test; (D) shows the duration of immobility in the tail suspension test; (E) shows the duration of grooming in the splash test. Data are represented as mean ± SEM of 6 to 16 mice per group, (*) $P < 0.05$, (**) $P < 0.01$, and (***) $P < 0.001$. Two-way ANOVA was followed by the Tukey multiple comparison test. ANOVA, analysis of variance; SNI, spared nerve injury.

and habituation to the arena for 5 consecutive days and before the habituation, respectively. For habituation, mice were placed into the empty arena (40 × 30 × 30 cm of width × length × height, versatile polyvinyl chloride) for 60 minutes. For NOR experiments, custom-built plastic pieces (polyoxymethylene) of different shapes (bell: 5 cm in diameter, 6 cm in height; diamond: 7 × 7 × 7 cm; and cube 5 × 5 × 5 cm) and same colour (black) or different colour and size (glass: 8.3 cm in diameter, 8.5 cm in height; cup: 6 cm in diameter, 6 cm in height) were used. The objects were cleaned thoroughly with 70% ethanol, followed by distilled water between trials to remove olfactory cues. During the sample phase on the first day of the NOR test, the mice were allowed to explore the 2 identical black objects (2 bells) for 6 minutes. For the short-delay test phase (1.5 hours), one of the sample objects (bell) was replaced by a new one (diamond), and exploration was measured for 5 minutes. For the long-delay test phase (24 hours), the new object was again exchanged by another new object. The location of the novel object at 24 hours was always different from that at 1.5 hours, either first left then right or vice versa. Consequently, the location of the familiar object also switched between the 2 test phases. Objects with the same colour but different shapes were considered to be similar to acquisition object.

Active exploration was defined as direct sniffing or whisking towards the objects or direct nose contact. Climbing over the objects was not counted as exploration. The relative exploration was quantified by normalizing the difference between the exploration time of the novel (Tn) and familiar object (Tf) by the total time of exploration (Ttot) to calculate the NOR discrimination index: NOR index = (Tn − Tf)/Ttot. With identical acquisition objects, the NOR index was always less than 0.2, indicating that there was no side preference in the mice used for the study.[12]

2.5.2. Y-maze test

To assess spatial memory, the Y-maze test was used. The apparatus consisted of 3 enclosed arms (30 × 5 × 15 cm; length × width × height) converging on an equilateral triangular center (5 × 5 × 5 cm). At the beginning of each experimental session, each mouse was placed in the center platform, and the number of spontaneous alternations (defined as the number of successive triplet entries into each of the 3 arms without any repeated entries) was monitored in a 5-minute test session. The percentage of alternation was calculated as the percentage of the ratio of the number of alternations/(total number of arm entries − 2).[56]

2.6. In vivo electrophysiological recording of long-term potentiation

In brief, mice were first anesthetized with urethane (1.5 g/kg, i.p.) and fixed in a stereotaxic device (David Kopf Instruments, Tujunga, CA). Body temperature was maintained at 37°C with a temperature-controlled heating pad (Harvard Apparatus Limited, Edenbridge, Kent). Extracellular field recording of LTP was performed contralateral to the operated hind paw at 1 month and 12 months after surgery. For LEC-DG pathway recording, the skull was exposed, and a hole was drilled for the placement of a recording electrode into the DG (AP: −2.1 mm from bregma, L: 1.5 mm from

midline; and V: 1.2 mm below dura) and a stimulating electrode into the LEC (AP: −4.0 mm from bregma; L: 4.5 mm from midline; and V: 2.9 mm below the dura). The stimulating and recording electrodes were lowered slowly into the LEC and DG, respectively, until a field excitatory postsynaptic potential (fEPSP) induced by test pulses (0.2 ms in duration delivered at the frequency of 0.033 Hz) was observed. After stabilization of the responses, a baseline was recorded for 30 minutes, and a high-frequency stimulation (TBS, consisting of 6 trains, 6 bursts, and 6 pulses at 400 Hz; interburst interval: 200 ms; and intertrain interval: 20 seconds) was applied in the LEC to stimulate the perforant path fibers for inducing LTP.[13] Long-term potentiation was considered as an increase in the amplitude and slope of the fEPSPs that exceeded the baseline by 20% and lasted for at least 30 minutes from the TBS. After TBS, the recording of the fEPSPs was continued for 90 to 120 minutes. Field recordings were performed with a tungsten microelectrode (1–5 Mohm), and EPSPs were recorded at 20 kHz every 30 seconds for 60 minutes. In addition, the excitatory responses were amplified (×100), filtered at 5 kHz, and digitized by an interface (Digidata 1320A, Axon Instruments, Indonesia) connected to a computer on which the analysis software (WinLTP 2.10) was installed. At the end of experiments, mice were euthanized with lethal dose of urethane, and the brains were removed. After fixation, the brains were cut into 40-μm thick slices and observed under a light microscope to identify the electrode locations. Animals showing an incorrect electrode place were discarded. The histological analysis of electrode placement was performed to further confirm the functional response obtained after paired-pulse facilitation application in the LEC. In particular, 2 subsequent pulses at an intensity value below the population spike threshold (between 20 and 120 μA/0.2 ms) with interpulse intervals varying from 15 to 100 milliseconds were applied. Six paired-pulse responses at each interpulse interval were collected and averaged, and the percentage of facilitation was calculated as relative potentiation of the second fEPSP to the first fEPSP.

For PFC-NAcore pathway, a bipolar stimulating electrode was placed into the prelimbic medial prefrontal cortex (PL-PFC) (anteroposterior [AP] +1.98 mm; mediolateral [ML] +0.3 mm; dorsoventral [DV] −2.3 mm from the brain surface), whereas tungsten recording electrode (1-5 Mohm) was lowered into the NAcore (AP + 0.98 mm, L ± 1 mm, DV − 3.5-4 mm from brain surface). Field recordings were acquired and analyzed with WinLTP software. Field potential amplitude (estimated as described earlier[59]) was stimulated at 40% of the minimum current intensity that evoked a maximum field response (from an input/output curve) every 30 seconds and then averaged every 1 minute to record a baseline for 20 minutes. After stabilization of a response, the LTP protocol was induced with high-frequency stimulation consisting of 2 bursts of 100 pulses at 50 Hz with a 20-second interburst interval.[59] The data were normalized to baseline field amplitude for each group and analyzed by using a 2-way analysis of variance (ANOVA) for repeated measures, followed by post hoc test.

2.7. Microdialysis

Microdialysis experiments were performed in awake and freely moving mice. In brief, mice were anaesthetized with pentobarbital (50 mg/kg, i.p.) and stereotaxically implanted with concentric microdialysis probes into the DG using the coordinates: AP: −2.1 mm from bregma, L: 1.5 mm from midline, and V: 1.2 mm below dura. Dialysis probes were constructed with 25 G (0.3 mm inner diameter, 0.5 mm outer diameter) stainless steel tubing (A-M Systems, Sequim, WA). Inlet and outlet cannulae (0.04 mm in inner diameter, 0.14 mm in outer diameter) consisted of fused silica tubing (Scientific Glass Engineering). The probe had a tubular dialysis membrane (Enka AG, Wuppertal, Germany), which was 1.3 mm in length. After a recovery period of 24 hours, dialysis was commenced with ACSF (NaCl 147 mM, $CaCl_2$ 2.2 mM, and KCl 4 mM; pH 7.2) perfused at a rate of 1 μL/minute by a Harvard Apparatus infusion pump. After a 60-minute equilibration period, 6 consecutive 30-minute dialysate samples were collected. At the end of experiments, mice were anaesthetized, and their brains were perfused and fixed through the left cardiac ventricle with heparinized paraformaldehyde saline (4%). The brains were dissected out and fixed in a 10% formaldehyde solution for 2 days. The brain was cut into 40-μm thick slices and observed under a light microscope to identify the probe locations. Dialysates were analyzed through a high-performance liquid chromatography method. The system comprised a Varian ternary pump (mod. 9010), a C18 reverse phase column, a Varian refrigerated autoinjector (mod. 9100), and a Varian fluorimetric detector. Dialysates were precolumn derivatized with o-pthaldialdehyde-N-acetylcysteine (OPA-NAC) (10 μL of dialysate + 5μL of OPA-NAC + 10 μL of 10% borate buffer), and amino acid conjugates were re-solved using a gradient separation. The mobile phase consisted of 2components: (1) 0.2 M sodium phosphate buffer and 0.1 M citric acid (pH 5.8) and (2) 90% acetonitrile and 10% distilled water. Gradient composition was determined using an Apple microcomputer installed with Gilson gradient management software. Data were collected using a Dell Corporation PC system 310 interfaced to the detector through a Drew data collection unit. The mean dialysate concentration of amino acids in the 6 samples represented the basal release, and the results were expressed as the mean ± SEM of the pmol in 10 μL of perfusate.

2.8. Gene expression analysis

2.8.1. RNA extraction and cDNA synthesis

Total RNA was isolated from either hippocampus or prefrontal cortex tissues of 4 groups of samples including the 12-month sham, 1-month sham, 12-month SNI, and 1-month SNI mice. TRIzol Reagent (Invitrogen, Carlsbad, CA) was used according to manufacturer's protocol. RNA was finally eluted into 20 μL of 0.1 mM EDTA buffer to concentrate the extract. RNA purity and quantity were measured by NanoDrop ND-1000 spectrophotometer (Thermo Scientific, Wilmington, NC) using the 260/280 ratio. RNA samples were stored at −80°C until further processing. The cDNA synthesis was performed using a High-Capacity cDNA Reverse Transcription Kit (Applied Biosystems, Carlsbad, CA).

2.8.2. Gene expression array

Equal amounts of cDNA from each group of mice were mixed to obtain 4 pools in duplicate for both the brain areas. In detail, each pool included 5 cDNA samples from either the 1-month mice or the 12-month mice, both for sham and SNI mice. The gene expression profiling was performed using TaqMan Array Mouse Immune Panel (Applied Biosystems), which allows simultaneous detection of 96 genes, including cytokines, chemokines, growth factors, and other immune response genes, and TaqMan Universal PCR Master Mix (Applied Biosystems) following manufacturer's manuals. The Ct values were determined using ViiA 7 software (Applied Biosystems) and setting a threshold of 0.2. The Ct values above 32.0 were set as undetermined. The relative quantification of each mRNA was calculated with the ΔΔCt method and fold change (FC) with the equation $2^{-\Delta\Delta Ct}$. The Ct values of each mRNA was normalized by GAPDH endogenous control, and the mean Ct values of an mRNA across 4 replicates

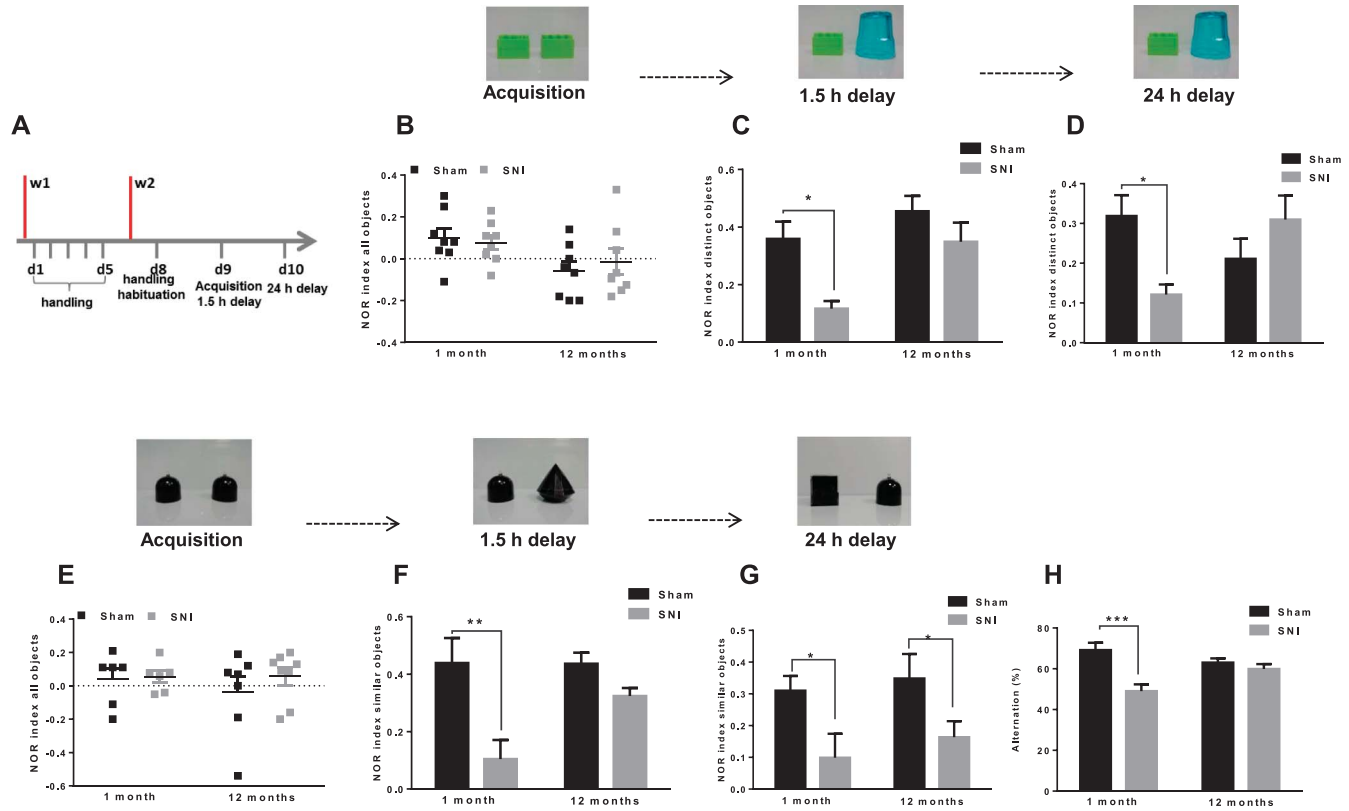

Figure 2. Effects of short-lasting and long-lasting SNI on cognitive performance. (A) Shows timeline of the experimental procedure in NOR. (B-D) Show NOR index and images of different objects in the object recognition protocol during acquisition, 1.5-hours and 24-hours delay, respectively, in the 1-month and 12-month SNI mice. (F-G) Show NOR index and images of similar objects in the pattern separation protocol during acquisition, 1.5-hour and 24-hour delay, respectively, in the 1-month and 12-month SNI mice. (H) Shows the percentage of the alternation in the Y-maze test in the 1-month and 12-month SNI mice. Data are represented as mean ± SEM of 8 mice per group, (*) $P < 0.05$ and (**) $P < 0.01$. After normality test for distribution evaluation, the Welch *t* test or ANOVA was assessed. The Tukey test was used for multiple comparisons. ANOVA, analysis of variance; NOR, novel object recognition; SNI, spared nerve injury.

for each pool were used. Transcripts with more than 2.5-fold difference in expression level were defined as differentially expressed. Differential expression of genes was assessed by linear regression models with empirical Bayes moderated t-statistics using Bioconductor package limma v.3.32.8. To account for multiple testing, false discovery rate (FDR)-adjusted *P* values were computed according to the Benjamini–Hochberg method. Comparison between 2 groups was analyzed with the Student *t* test. Heatmap was constructed using the statistical computing tool GraphPad Prism software (v7.05).

2.8.3. Gene list analysis

The publicly available algorithm PANTHER (Protein ANalysis THrough Evolutionary Relationships) (v16.0) is a classification system designed to classify proteins (and their genes) to facilitate high-throughput analysis (http://www.pantherdb.org). We used this tool for pathway enrichment analysis of differentially expressed genes.

2.9. Regulatory T lymphocyte evaluation

Regulatory T lymphocytes (Treg) percentage was analyzed in the 1-month and 12-month SNI mice. In brief, blood samples (200 μL) were collected in sterile EDTA vacutainers. Peripheral blood samples (50 μL) were incubated with a monoclonal antibody cocktail for detecting regulatory T cells: APC-H7-conjugated anti-CD4, APC-conjugated anti-CD25, FITC-conjugated anti-CD127, and PerCP-cy5.5 conjugated anti-CD45 for 30 minutes at 4°C. After incubation, blood samples were treated with 2 mL of FACS lysing solution (BD Biosciences) for 10 minutes at room temperature in dark, washed with PBS, acquired on an FACS Canto flow cytometer, and analyzed with Diva software (BD Biosciences). The regulatory T lymphocytes showed a phenotype as $CD4^{+}CD25^{+}CD127^{low/-}$.

3. Results

3.1. Spared nerve injury induces mechanical and thermal allodynia

Spared nerve injury of the sciatic nerve decreased the ipsilateral paw nociceptive threshold (PWT) to mechanical and thermal stimuli. Indeed, SNI procedure caused a significant reduction of the PWT in the ipsilateral hind paw (sham mice: 0.7275 ± 0.134 g; SNI mice: 0.04188 ± 0.0092 g; $P < 0.0001$) 1 month after nerve damage. Similarly, 12 months post-SNI, operated animals presented a decreased threshold when compared with controls (sham mice: 0.8475 ± 0.1428 g; SNI mice: 0.0735 ± 0.01374 g; $P < 0.001$) (**Fig. 1B**). We did not find any difference in mechanical threshold in the contralateral mice paw (data not shown).

Likewise, after acetone administration, the number of flickering and lickings was significantly higher in SNI mice (SNI mice: 1.333 ± 0.2 after 1 month and 2.039 ± 0.348 after 12 months) when compared with sham animals (sham mice: 0.1667 ± 0.10 after 1 month and 0.5171± 0.1 after 12 months, $P = 0.0124$ and $P = 0.0005$, respectively) (**Fig. 1C**). Accordingly, the latency to the

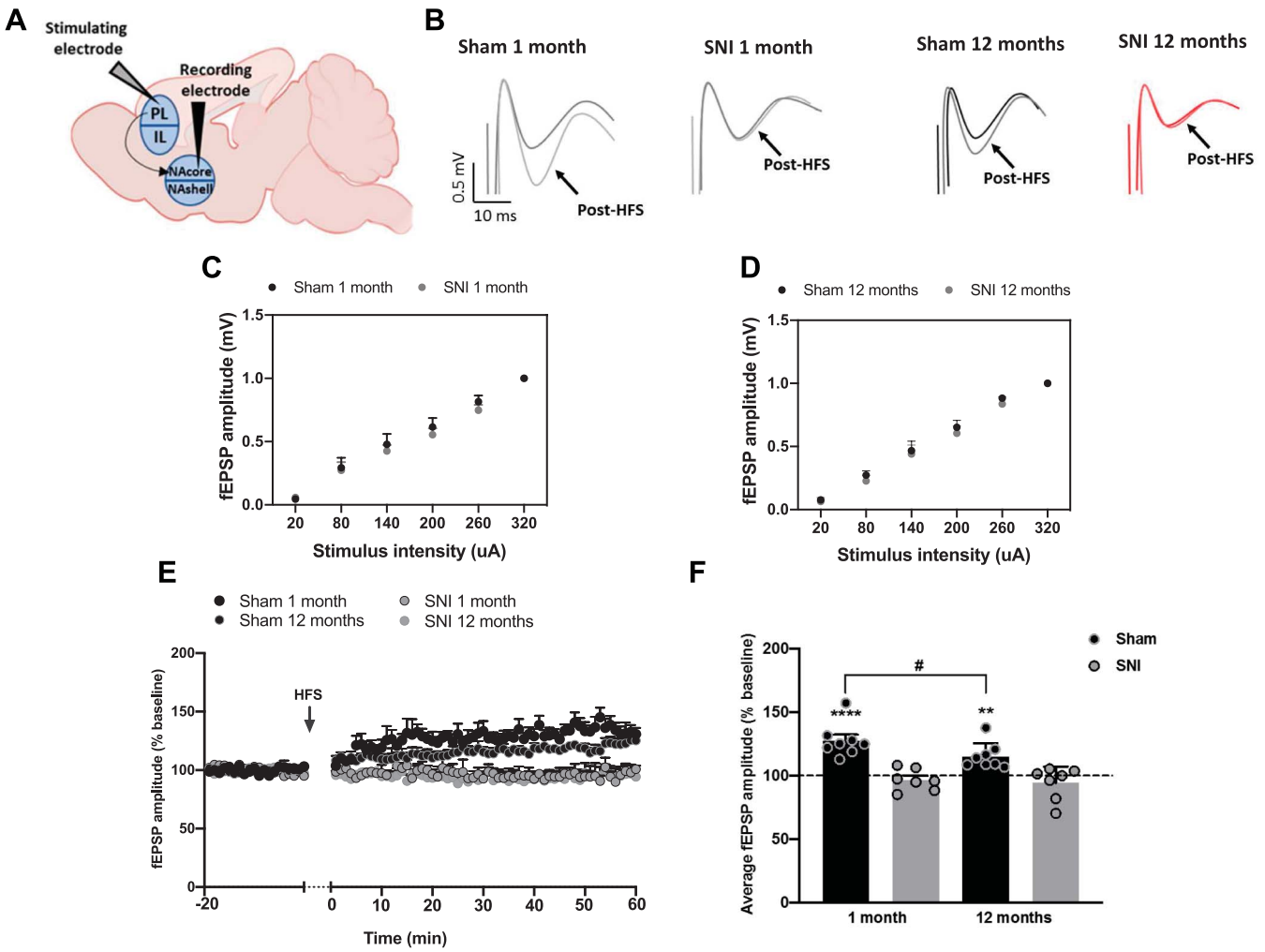

Figure 3. Long-term potentiation at the PL-NAcore pathway in sham and SNI mice 1 month and 12 months after injury. (A) Shows a simplified schematic PL-NAcore pathway for in vivo extracellular LTP recording. (B) Shows traces of the amplitude of the fEPSP recorded in Nacore in each group. (C) Shows input–output curves constructed from the fEPSP amplitude vs increasing stimulation intensities at the PL in the 1-month sham and SNI mice. (D) Shows input–output curves constructed from the fEPSP amplitude vs increasing stimulation intensities at the PL in the 12-month sham and SNI mice. (E) Data points were normalized by the mean field amplitude observed during the baseline period (20 minutes before HFS). At arrow, HFS was delivered, and changes of the fEPSP amplitude were recorded over the 60 minutes after HFS. (F) Shows the mean ± SEM of the average field amplitude over the 60 minutes after HFS. *Indicates significant differences vs pre-HFS (0-20 minutes); #indicates significant differences between sham groups. fEPSP, field excitatory postsynaptic potential; HFS, high-frequency stimulation; SNI, spared nerve injury; LTP, long-term potentiation.

withdrawal was reduced in both the 1-month and 12-month SNI mice compared with the related controls (not shown). No difference in pain behaviors was observed in contralateral paw in all groups of animals (not shown).

3.2. Spared nerve injury induces depressive-like behaviors

Neuropathy induces an anxiodepressive phenotype in mice.[34] In this study, the time of immobility in the tail suspension test was significantly higher in SNI mice when compared with control animals at 1 and 12 months after nerve injury (SNI mice: 88.21 ±6.3 seconds after 1 month and 96.41 ± 6.75 seconds after 12 months and sham mice: 57.88 ±4.8 seconds after 1 month and 67.50 ± 6.591 seconds after 12 months; $P = 0.0061$ and $P = 0.0085$, respectively), suggesting a marked reluctance to maintain an active escape-oriented behavior in an advanced state of neuropathy (**Fig. 1D**). In the splash test, SNI mice showed a decrease in the duration of grooming activity between groups (SNI mice: 86.38 ± 5.539 seconds after 1 month and 53.00 ± 5.9 seconds after 12 months and sham mice: 123 ± 9.2 seconds after 1 month and 89.30 ± 7.1 second after 12 months; $P = 0.0019$ and $P = 0.0125$, respectively). A slight but significant ($P = 0.0149$) reduction in the grooming activity was recorded in the 12-month sham mice when compared with the 1-month ones (**Fig. 1E**). The wire hang test and rotarod test indicated that the muscle strength and motor functioning were not compromised by SNI (not shown).

3.3. Spared nerve injury affects object recognition memory

We have previously showed that SNI causes significant impairments in memory functioning in mice.[10,56] In this study, in the 1-month and 12-month SNI animals, we assessed learning and long-term memory in the NOR test by testing the capability of animals of mnemonic discrimination of dissimilar (recognition memory) and similar (pattern separation) objects (**Fig. 2A**). In the acquisition phase, animals were exposed to 2 identical objects with the same colour, size, and shape. The total exploration time during the acquisition phase was not affected by SNI condition (SNI mice: 42.16 ± 0.05 and sham mice: 38.98 ± 0.04 at 1

month; SNI mice: 37.6 ± 0.08 and sham mice: 40.1 ± 0.09 at 12 months). Both the 1-month sham and 1-month SNI mice had the exploration time less than 0.2, indicating that there was no side preference. However, exchanging one of the objects by a novel (dissimilar) object induced a significant side preference towards the novel object in the 1.5-hour and 24-hour delay test phases (SNI mice: 0.1163 ± 0.02 and 0.1213 ± 0.02 at 1.5 hours and 24 hours, respectively; sham mice: 0.3588 ± 0.06 and 0.3188 ± 0.05, at 1.5 hours and 24 hours, respectively) ($P = 0.0173$ and $P = 0.0379$) (**Fig. 2B–D**). Likewise, when using a similar object with the same colour (but different shape), SNI animals showed a reduced discrimination index when compared with the control animals (SNI mice: 0.104 ± 0.06 and 0.0987 ± 0.07 at 1.5 hours and 24 hours, respectively; sham mice: 0.4386 ± 0.08 and 0.3100 ± 0.04 at 1.5 hours and 24 hours, respectively) ($P = 0.01$ and $P = 0.018$) (**Fig. 2E–G**). These data indicated that 1 month after SNI surgery, animals were not perfectly able to distinguish neither similar nor dissimilar objects during both short-term and long-term retention tests. One year after nerve damage, in the presence of dissimilar objects, animals presented a normal recognition index when compared with related controls (SNI mice: 0.348 ± 0.06 and 0.310 ± 0.06 at 1.5 hours and 24 hours, respectively; sham mice: 0.455 ± 0.05 and 0.2110 ± 0.05 at 1.5 hours and 24 hours, respectively) (**Fig. 2B–D**). Instead, with similar objects, SNI mice were not able to remember which of the objects was familiar and which was novel (SNI mice: 0.3238 ± 0.02 and 0.1643 ± 0.05 at 1.5 hours and 24 hours, respectively; sham mice: 0.436 ± 0.03 and 0.3488 ± 0.07 at 1.5 hours and 24 hours, respectively) ($P = 0.06$ and $P = 0.03$) (**Fig. 2E–G**). These data indicated that 12 months after SNI surgery, animals can distinguish dissimilar, but not similar objects.

3.4. Spared nerve injury affects spatial working memory

In accordance with our previous data,[56] 1 month after SNI, mice showed memory impairments in the Y-maze test, as indicated by a significant ($P = 0.0002$) decrease in the percentage of alternations (49.05 ± 3.293%) compared with sham animals (69.19 ± 3.5%) (**Fig. 2H**). Of interest, in the 12-month SNI mice, we did not observe significant ($P = 0.8710$) changes in the spontaneous alteration between arms (59.88 ± 2.41%) compared with the related control group (63.00 ± 2.079%) (**Fig. 2H**), suggesting a regular spatial working memory.

3.5. Spared nerve injury affects synaptic plasticity in the prefrontal cortex projection to the nucleus accumbens core

The PFC projects to the NAcore by driving reward-associated behaviors.[38] In fact, this pathway has also been shown to be involved in pain processing by regulating the transition from acute to chronic pain.[49] However, it has not yet been investigated whether this circuit may play a role in the neurological consequences of neuropathic pain. To address this question, we evaluated the synaptic plasticity in the PFC-NAcore synapses in mice with short-term and long-term neuropathy (**Fig. 3A**). No differences were observed in input–output curve between SNI and sham mice both at 1 and 12 months (**Fig. 3B–D**, respectively). High-frequency stimulation delivered to the PFC (PL-PFC) induced a significant potentiation of NAcore EPSPs amplitude in the 1-month (20-80 minutes: 127.77 ± 4.69%, $P < 0.0001$) and 12-month (20-80 minutes: 115.46 ± 3.63%, $P = 0.0015$) sham mice (**Fig. 3E and F**). In particular, the magnitude of LTP in 1-month sham mice resulted slightly greater than that observed in the 12-month mice ($P = 0.0193$). Intriguingly, impaired LTP was found in mice with 1 month and 12 months of neuropathy. Indeed, PL-PFC high-frequency stimulation failed to induce LTP in the core region of the nucleus accumbens in the 1-month and 12-month SNI mice (96.82 ± 3.21% and 94.39 ± 4.95%, respectively) (**Fig. 3E and F**). A 2-way ANOVA for repeated measures, followed by the Tukey test revealed a significant effect of time ($F[1,26] = 16.53$, $P = 0.0004$), a significant effect of disease model ($F[3,26] = 14.31$, $P < 0.0001$), and a significant interaction time × disease model ($F[3,26] = 14.36$, $P < 0.0001$). Correlation of field postsynaptic excitatory responses and behaviors (NOR test and tail suspension) is given in Figure S1 (available at http://links.lww.com/PAIN/B547).

3.6. Spared nerve injury affects synaptic plasticity at the lateral entorhinal cortex-dentate gyrus pathway

To investigate the impact of the timing of neuropathy on hippocampal long-term synaptic plasticity, we analysed the LEC-DG LTP in the 12-month SNI mice (**Fig. 4A and B**). Synaptic maladaptive changes in the LEC-DG circuit have been previously correlated with the reduced cognition in 30-dayneuropathic mice.[10] In agreement, the TBS application in the LEC significantly potentiated amplitude (30-60 minutes: 238.82 ± 22.50%, $P < 0.0001$, $t21 = 31.33$) (Fig. S2, available at http://links.lww.com/PAIN/B547) and slope (30-60 minutes: 222.93 ± 14.49%, $P < 0.0001$, $t21 = 65.10$) (**Fig. 4C and D**) of the fEPSPs in the DG in sham mice. Moreover, SNI condition completely inhibited LTP induction. Indeed, 1-month SNI mice did not show any change of the fEPSPs amplitude (Fig. S2, available at http://links.lww.com/PAIN/B547) (30-60 minutes: 103.06 ± 4.40%; $P = 0.40$, $t21 = 0.84$) and slope (30-60 minutes: 103.7 ± 6.2%, $P = 0.19$, $t21 = 1.33$) (**Fig. 4C and D**) after TBS application, as assessed by unpaired *t* test. As previously observed, 1-month SNI mice input–output curves shifted leftwards in both amplitude (Fig. S2, available at http://links.lww.com/PAIN/B547) and slope parameters (**Fig. 4B and C** left panel) when compared with 1-month sham mice, whereas no differences were observed in input–output curve in both amplitude (Fig. S2, available at http://links.lww.com/PAIN/B547) and slope parameters (**Fig. 4B and C** right panel) between the 12-month SNI and 12-month sham mice. Of interest, the 12-month SNI animals showed a partial reestablishment of the DG synaptic responses for amplitude (151.26 ± 20.39%, $P < 0.001$, $t21 = 36.63$) (Fig. S2, available at http://links.lww.com/PAIN/B547) and slope (189.40 ± 15.09%, $P < 0.0001$, $t21 = 28$) (**Fig. 4B and D** left and right panels) detected after TBS application. Finally, 2-way ANOVA analysis for repeated measures has identified significant effect for treatment ($F[59,600] = 512.9$, $P < 0.0001$), for time ($F[2,600] = 8.0$, $P < 0.0001$) and interaction treatment × time ($F[118,600] = 3.22$, $P < 0.0001$) for amplitude factor. Similarly, significant effect for treatment ($F[59,600] = 10.79$, $P < 0.0001$), time ($F[2,600] = 397.88$, $P < 0.0001$), and interaction treatment X time was observed ($F[118,600] = 2.64$, $P < 0.0001$) for slope factor. Correlation of field postsynaptic excitatory responses and behaviors (NOR test and tail suspension) is given in Figure S1 (available at http://links.lww.com/PAIN/B547).

3.7. Spared nerve injury effects on extracellular amino acids levels in the dentate gyrus

Extracellular amino acids levels in the DG of the 12-month sham and SNI mice were measured by in vivo microdialysis associated with HPLC (**Fig. 4**). SNI mice showed a significant ($P < 0.001$) increase in GABA levels (14.53 ± 2.1 pmol/μL) compared with sham animals (5.669 ± 0.71 pmol/μL) (**Fig. 4E**). The levels of extracellular L-glutamate (Glu); D-aspartate (Asp); glycine (Gly)

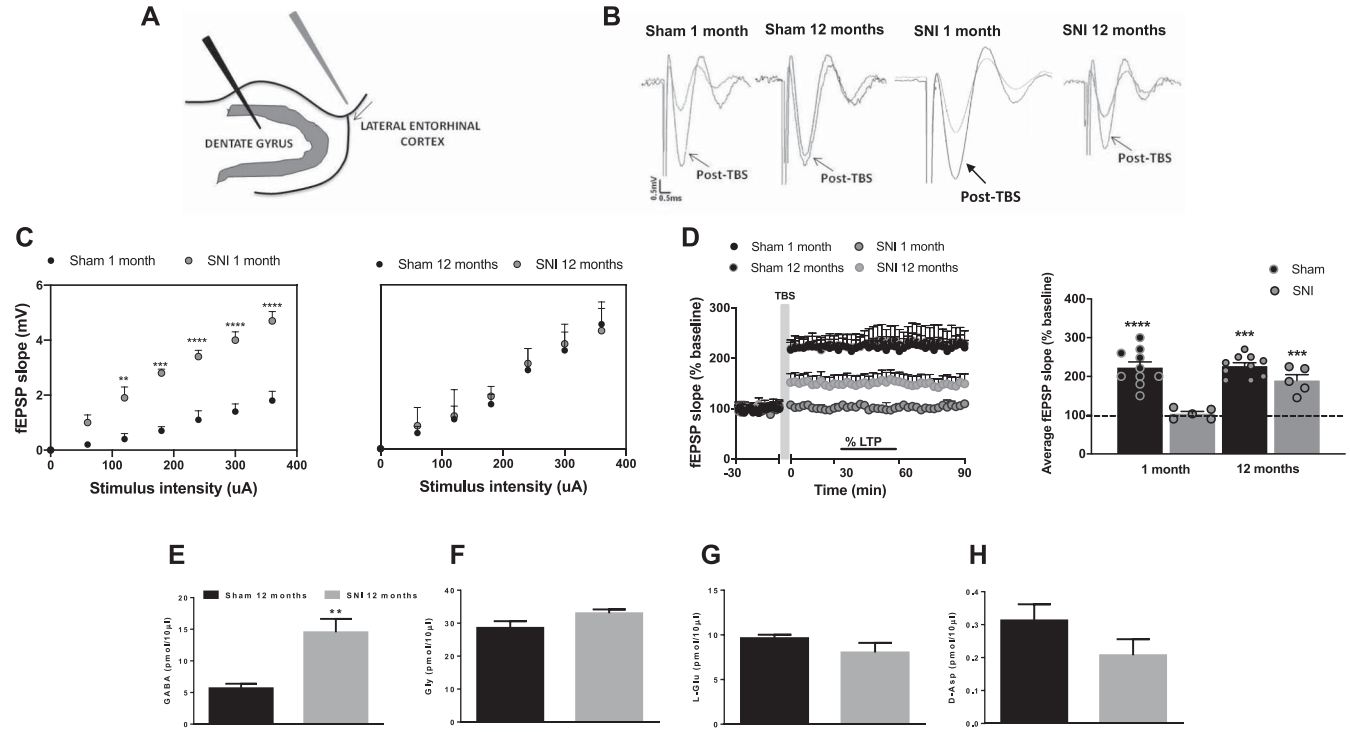

Figure 4. Long-term potentiation at the LEC-DG pathway in sham and SNI mice 1 month and 12 months after injury. (A) Shows the diagrammatic representation of the placement of the stimulating electrode in the LEC for stimulating the lateral perforant path (LPP) fibers and of the recording electrode in the DG for recording the fEPSPs of granular cells. (B) Shows sample traces of a single evoked fEPSP recorded in the DG before and after TBS application in the 1-month and 12-month sham or SNI mice. (C) Shows input–output curves constructed from the fEPSP slope vs increasing stimulation intensities at the LEC in the 1-month and 12-month sham and SNI mice (left and right, respectively). (D) Shows time-dependent changes in the fEPSP slope after TBS application normalized to basal responses in the 1-month and 12-month sham or SNI mice. Data are represented as mean ± SEM of fEPSPs slope. $^{**}P < 0.01$, $^{***}P < 0.001$, and $^{****}P < 0.0001$ indicate significant differences vs pre-TBS (15-30 minutes). $P < 0.05$ was considered statistically significant. The extracellular level GABA (E), Glycine (F), L-Glutamate (G), and D-Aspartate (H) are shown in the DG of the 12-month sham and SNI mice. Data are shown as the mean ± SEM (pmol/10 µL). **Indicates significant differences vs the 12-month sham mice. Two-way ANOVA was followed by the Tukey multiple comparison test. ANOVA, analysis of variance; fEPSP, field excitatory postsynaptic potential; LEC-DG, lateral entorhinal cortex-dentate gyrus; SNI, spared nerve injury.

were not significantly changed 12 months after surgery in SNI mice when compared with those in related controls (SNI mice: 8.029 ± 1 pmol/µL and sham mice: 9.625 ± 0.3 pmol/µL; SNI mice:0.2073 ± 0.04 pmol/µL and sham mice: 0.3127 ± 0.04 pmol/µL; SNI mice: 33.02 ± 1.16 pmol/µL and sham mice: 28.58 ± 2.039 pmol/µL, for L-Glu, D-Asp, and Gly, respectively) (**Fig. 4F–H**).

3.8. Spared nerve injury corresponds with distinct proinflammatory altered gene expression patterns in the prefrontal cortex and hippocampus

We next investigated whether SNI was associated with changes in gene expression in the brain regions known to be involved in affective components of chronic pain. The expression levels of 96 genes, including cytokines, chemokines, growth factors, and several markers, were analysed in both hippocampus and PFC of the 1-month and 12-month SNI mice and related controls (**Figs. 5 and 6**). In detail, tissue samples were pooled for each category based on the brain area, age, and condition and then processed for mRNA microfluidic TaqMan array using Mouse Immune Panel. The relative gene expression in the 1-month and 12-month sham mice revealed 34 more than 2.5-fold upmodulated genes in hippocampus and 15 ones in PFC (**Fig. 5A and B**). Data elaboration by PANTHER classification system revealed, for the hippocampal pattern, 8 genes sharing a common involvement in inflammation mediated by either chemokine or cytokine signaling pathway (Fig. S3A, available at http://links.lww.com/PAIN/B547). Among these, in addition to proinflammatory chemokines and cytokines Chemokine (C-C motif) ligand 19 (CCL19); C-X-C motif chemokine ligand 10 (CXCL10); Interleukin-15 (IL-15); Interleukin-18 (IL-18) (CCL19, CXCL10, IL15, and IL18), stands out the 5.1 and 14.9 upregulation of nuclear factor NF-kappa-B (NFKB1) and inhibitor of nuclear factor kappa B kinase subunit beta (IKBKB), respectively. Pathway enrichment analysis also revealed the involvement of 5 genes in apoptosis signaling pathway, 4 genes in cholecystokinin receptor (CCKR) signaling pathway, and 3 genes in JAK/STAT pathway. Among the most regulated genes, we also observed β2-microglobulin (B2M, 10.6-fold), the complement component C3 (23.8-fold), CC chemokine receptor 2 (CCR2, 8.3-fold), CD38 (15.4-fold), H2-Eb1 (16.3-fold), hypoxanthine phosphoribosyltransferase 1 (HPRT1) (26.6-fold), leucocyte marker PTPRC (CD45, 13.6-fold), and suppressor of cytokine signaling 2 (SOCS2) (39.5-fold).

Of note, 11 genes resulted commonly upregulated to a significant extent both in the hippocampus and in PFC of the 12-month sham mice compared with the 1-month ones (**Fig. 5C**). On the other hand, the proinflammatory cytokines CCL2, CCL5, and IL12A, as well as the costimulator of T-cell activation and proliferation CD86, were upregulated only in the cortex of the 12-month sham mice compared with the 1-month ones (**Fig. 5D and E**). The PANTHER software analysis displayed the prominent modulation of inflammation mediated by chemokine and cytokine signaling pathways and T-cell activation (Fig. S3B, available at http://links.lww.com/PAIN/B547).

Overall, these data demonstrate the existence of an enhanced neuroinflammation status in old brain, as demonstrated by the higher

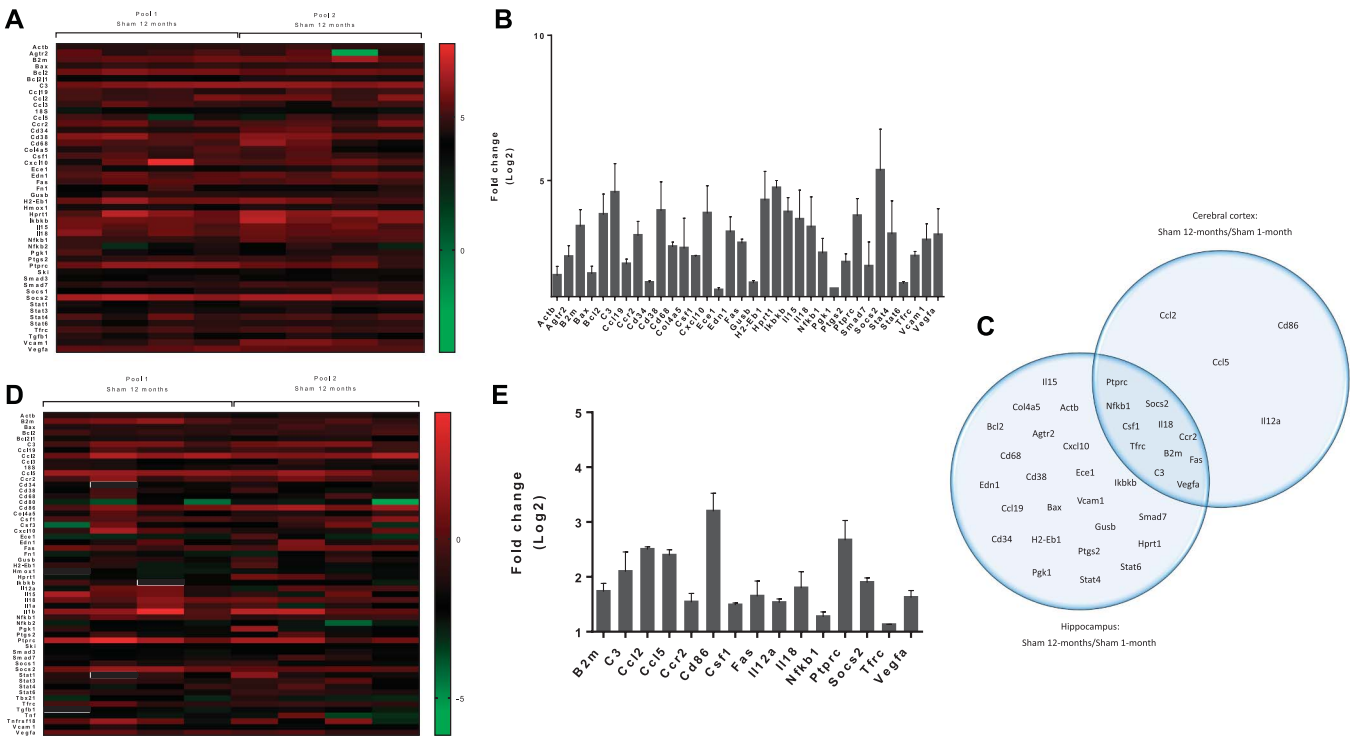

Figure 5. Gene expression profile in hippocampus and PFC of sham mice at 12 months compared with the 1-month animals. (A and D) Show the heatmap summarizing the global and distinct gene expression levels across the screening sets in hippocampus (A) and PFC (D), profiled by the results of low-density TaqMan-RT-qPCR array. The analysis was performed using GraphPad Prism software (version 7.05). (B and E) Show the expression levels of the significantly ($P < 0.05$) deregulated genes between sham mice at 12 months and at 1 month in hippocampus (B) and PFC (E). Data are expressed as the mean ± SD. (C) Shows the Venn diagram representing the cross-comparison of deregulated genes within the screening sets. PFC, prefrontal cortex.

amount of proinflammatory and stress-associated mediators in older mice compared with the younger ones. Moreover, these factors are mainly expressed in the hippocampal region compared with the cortex. The same pattern of genes was analysed to compare sham and SNI mice coupled on the basis of brain area and injury duration (**Fig. 6**). As a result, we observed the significant upregulation of 26 genes in the hippocampus of the 1-month SNI mice compared with the 1-month sham animals (**Fig. 6A and B**). Among these genes, there are the apoptosis-related factors Bax and Bcl-2 (3.4 and 4.3-fold), the endothelial marker CD34 (3.4-fold), the pan-macrophage marker CD68 (3.4-fold), the ADP-ribosyl cyclase CD38 (3.6-fold), which acts as a regulator of neuroinflammatory processes in astrocyte-induced neuroprotection,[35] CCR2 (4.3-fold), and macrophage colony-stimulating factor-1 (4.4-fold). A substantial upregulation of the proinflammatory cytokines IL18, IL1B, and IL7 (2.6-fold, 3.5-fold, and 9.6-fold, respectively) was also recorded, together with the inflammatory mediators PTGS2, NFkB1 and 2, STAT6, and IKBKB by 2.7-fold, 5.0-fold, 2.5-fold, 3.3-fold, and 6.9-fold, respectively. The activation of the classical pathway of the complement system was also revealed by 5.3-fold upregulation of C3 gene. A possible rebound effect of these multiple proinflammatory stimuli could be the reason for the huge increase of SOCS2 expression (11.1-fold). The immunosuppressive cytokine TGF-β1, which acts as a pivotal controller of cell growth and differentiation and of tissue repair after injury,[62] was upregulated by 3.2-fold, but a simultaneous induction of its negative regulator SMAD7 (3.7-fold) was observed too. The expression of angiogenic factors EDN1 and VEGFA, as well as the adhesion molecule VCAM1, was also found strongly induced (3.6-, 6.5-, and 3.4-fold, respectively). Worthy of note is the huge induction of transferrin receptor (TFRC, 5-fold). The PANTHER software revealed the representation of the most affected pathways in the hippocampus of the 1-month SNI mice compared with the 1-month sham animals (Fig. S3C, available at http://links.lww.com/PAIN/B547), showing 8 genes involved in inflammation mediated by chemokine and cytokine signaling pathways, 5 genes in apoptotic pathway, 4 in CCKR map, other 4 in Toll receptor signaling pathway, and other genes variously involved in B-cell activation, T-cell activation, TGF-β, Wnt, PDGF, and endothelin signaling pathways.

The comparison between cortical tissues of the 1-month SNI and sham mice displayed the significant downmodulation of just one gene, the transcription factor TBX21 (3.4-fold) (**Fig. 6C and D**), a regulator of both innate and adaptive immunity through the modulation of Toll-like receptor 2 expression and T-cell homing to proinflammatory sites acting on CXCR3 expression.[43]

On the other hand, only few genes become substantially modulated in both hippocampus and PFC of the 12-month SNI mice compared with the respective sham animals. In detail, in the hippocampus, 2 genes endowed with opposite immunomodulatory effects were downregulated (**Fig. 6E and F**): CTLA4 (CD152, 3.6-fold) expressed on recently activated $CD4^+$ and $CD8^+$ T lymphocytes, with inhibitory signal,[17] and STAT4 (2.5-fold), which increases inflammation during protective immune response.[40] Regarding the cortical region, we found the following again: CTLA4 downmodulation (4.6-fold) and VCAM1 upregulation (2.8-fold) (**Fig. 6G and H**).

In conclusion, a substantial activation of both inflammatory and immune mediators was observed in the hippocampus of the 1-month SNI mice, thus reverting the basal immune profile detected in sham mice. Otherwise, only few mediators, but substantially directed towards a positive regulation of immune response, were observed in the PFC of both the 1-month and 12-month SNI mice.

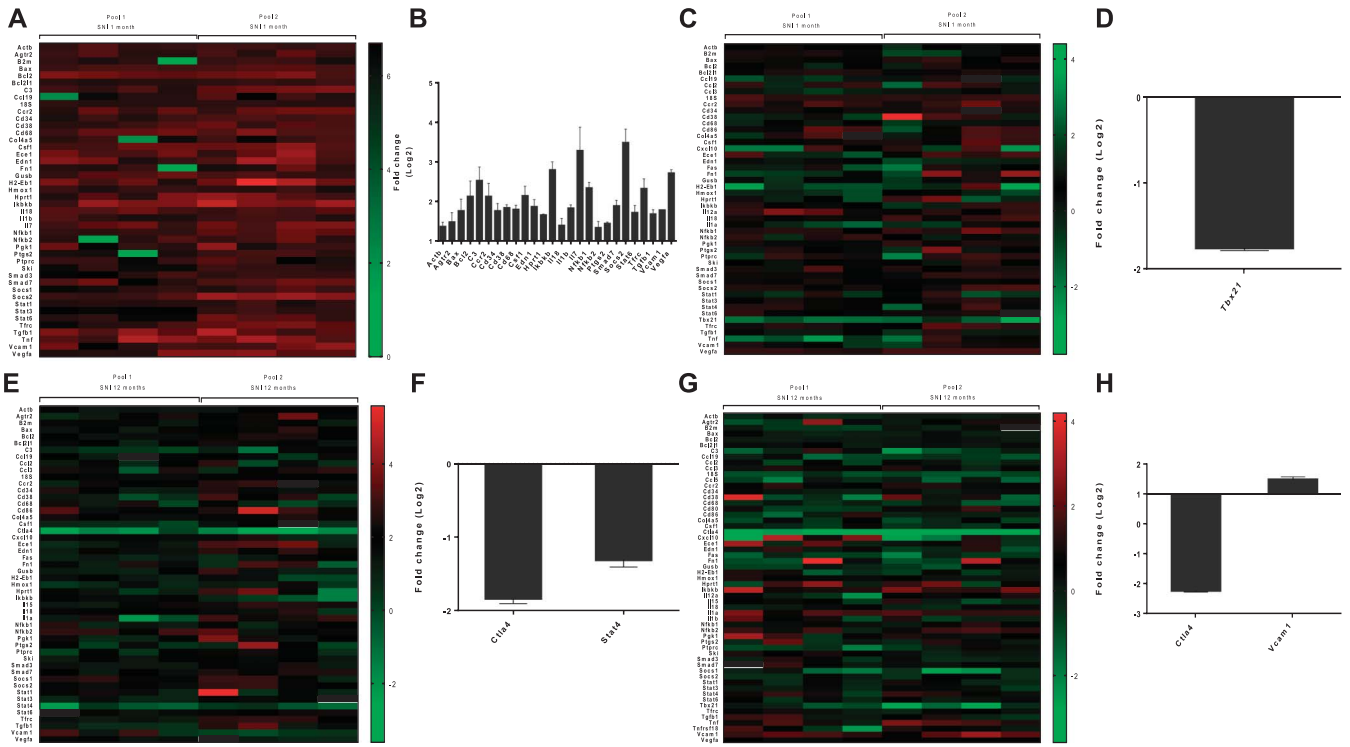

Figure 6. Gene expression profile comparison between SNI and sham mice coupled by brain area and injury duration. (A, C, E, and G) Show the heatmap summarizing the global and distinct gene expression levels across the screening sets in hippocampus (A) or PFC (C) of the 1-month SNI mice compared with sham animals and in hippocampus (E) or PFC (G) of the 12-month SNI mice compared with sham animals. The heatmaps were profiled based on the results of low-density TaqMan-RT-qPCR array, and the analysis was performed using GraphPad Prism software (version 7.05). (B, D, F, and H) Show the expression levels of the significantly ($P < 0.05$) deregulated genes between the 1-month SNI and sham mice at hippocampal region (B) or at PFC (D) and between the 12-month SNI and sham mice at hippocampal region (F) or at PFC (H). Data are expressed as the mean ± SD. PFC, prefrontal cortex; SNI, spared nerve injury.

3.9. Spared nerve injury does not affect the percentage of blood regulatory T cells

To gain more insight into the role of regulatory T cells in our model, we investigated the possible change in percentage of these cells in both the 1-month and 12-month neuropathic mice. Regarding the total T helper $CD4^+$ lymphocytes expressing CD25, we observed a significant ($P < 0.0001$) increase (5071 ± 1715%) in the 12-month sham mice when compared with the 1-month ones (1743 ± 0.1525%) (**Fig. 7A**). However, by comparing SNI with corresponding control groups, we did not detect any differences in the percentage of regulatory $CD4^+CD25^+CD127^{low/-}$ T lymphocytes, as well as in the percentage of total $CD4^+CD25^+$ T lymphocytes (**Fig. 7B**).

4. Discussion

The goal of this study was the phenotypic characterization of long-term SNI in mice. We coupled behavioral testing and in vivo electrophysiology to correlate behavioral deficits with specific circuit dysfunctions across PFC and limbic regions. Moreover, we evaluated the regulation of several genes involved in immune response and inflammation triggered by SNI. Data obtained at 1 year of neuropathy were compared with those relating to 1 month, which represent the most characterized SNI timing.

Studies based on animal models suggested the timing as a crucial factor in the development of the affective/cognitive disorders frequently associated with chronic pain. While pain symptoms develop immediately, such disturbances have been reported to emerge weeks or months after injury,[37,66] and sometimes, they persist after the resolution of painful hypersensitivity.[27,58] Thus, the precise onset and development of behavioral changes are highly dependent on the pain animal model used.

Our data confirmed that SNI model induces mechanical hypersensitivity, which is still evident 12 months after injury.[63] We did not observe any difference for pain responsiveness at mechanical or thermal (cold) stimuli between 1 and 12 months of SNI. Moreover, both groups of animals showed an enhanced immobility and reduced grooming activity, signs of behavioral despair, and anhedonia by resembling the lack of motivation or depression often observed in patients experiencing chronic pain. Such sickness behavior in SNI mice was not accompanied by an impaired motor coordination or spontaneous locomotory activity. Of interest, in the 12-month SNI mice, pain and depressive-like behaviors were not accompanied by cognitive impairments. Hypocognition and memory deficits, which represent major complications in patients with chronic pain, are well documented in short-term SNI.[34] Indeed, peripheral nerve injury may prompt reduced hippocampal synaptic plasticity across specific brain circuits regulating learning and spatial memory tasks.[3] We have previously shown that 30 days of SNI causes the abolishment of LTP at LEC-DG pathway. The loss of LTP, associated with a higher basal amplitude and slope in response to the single pulse, might probably be due to the increase in glutamate levels in the dentate gyrus.[10] Such functional and biochemical modifications could also be due, at least partly, to morphological reorganisation of the neuronal shape, as it has been reported for the prefrontal cortex pyramidal neurons in the same peripheral neuropathic pain model.[51] The morphological changes of the basal and apical dendrites in the SNI in both cortices and hippocampus,[51] might, in turn, drive the changes in the long-term potentiation, as previously demonstrated.[57]

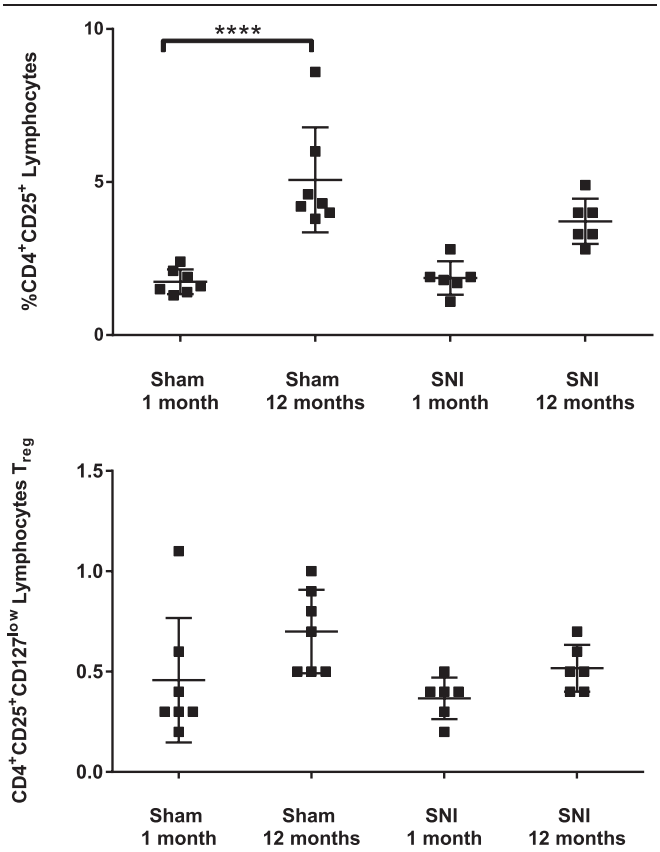

Figure 7. Analysis of the percentage of specialized subpopulation of regulatory T cells (Tregs) in sham and SNI mice 1 month and 12 months after injury. Panel shows changes in the of percentage of T $CD4^+$ lymphocytes expressing CD25 (A) and $CD4^+CD25^+CD127^{low/-}$ regulatory T lymphocytes (B) in the 1-month or 12-month SNI and sham mice. Values are expressed as the mean ± SEM of measurements of at least 3 independently performed experiments. Two-way ANOVA was followed by the Tukey multiple comparison test. ANOVA, analysis of variance; SNI, spared nerve injury.

We showed that spatial and discriminative memory was not impaired in the 12-month SNI mice, along with the physiological establishment of the hippocampal LTP. In the same animals, extracellular glutamate levels were unchanged, whereas gamma aminobutyric acid (GABA) levels resulted increased. These neurobiochemical data suggest that in the 12-month SNI mice, the oversensitization due to the glutamate spillover may be counterbalanced by an increased activity of the GABAergic terminals.

Specifically, we tested the effects of SNI on the pattern separation during the NOR test using similar or substantially dissimilar objects. Thirty-day injured mice exhibited recognition deficits, as shown by the disruption of NOR memory. This effect was not dependent on the relative similarity of the tested objects (pattern separation or NOR), indicating that SNI mice were not able to remember the shape of the objects they have seen the day before. On the contrary, the 12-month SNI mice showed a regular NOR and an unaltered spatial memory. These findings strengthen the concept that the disruption of LEC-DG circuitry may contribute, at least partly, to the cognitive impact of neuropathic pain. Of interest, the 12-month SNI mice showed an impaired pattern separation. It should be taken into account that pattern separation performances may gradually decline with the aging.[16,19] Through multiple mechanisms mainly in the DG and CA3 regions, separation performances have been correlated with adult DG neurogenesis.[4,64] It is known that the production of new DG neurons markedly decreases with age.[24,44] Thus, we cannot rule out that 1 year of SNI may worse the age-associated deficits or, alternatively, may negatively affect other structures regulating pattern separation ability in aged animals, ie, perirhinal cortex.[14,50]

It is known that reward circuitry components participate in depression and chronic pain mechanisms.[28] Indeed, stimulation of NAc has been correlated with the reduction of depressive symptoms of chronic pain.[30,61] In this study, we observed that both the 1-month and 12-month SNI mice showed impaired LTP in PFC-Nacore pathway. These data are compatible with recent findings showing that the deactivation of PFC-Nacore projection in rats induces an exacerbation of both sensory and aversive phenotypes of SNI.[68] Thus, we can speculate that the reduced synaptic plasticity in the PL projection to the NAcore may play a role in the affective consequences of SNI.

The immune system is deeply involved in neuropathic pain pathophysiology.[15,47] Previous studies suggested that the immune-neuronal communication initiated by proinflammatory mediators may participate to the sensorial components, as well as the affective components of neuropathic pain. Specifically, neuroinflammation, driven by changes in resident microglia and astrocytes, triggers neural reorganization believed to be responsible for cognitive deficit and depression after peripheral nerve injury.[5,46] In addition, depending on the nature of injury, T cells may contribute to the onset or the resolution of pain.[42] Regarding the SNI model, while Costigan et al.[21] have suggested the role of peripheral T cells in the spinal pain processing, another study indicated that there is not a relevant T-cell infiltration.[29] Our data indicate that 1 or 12 months of SNI does not affect the percentage of circulating regulatory T cells. However, further analysis is needed to evaluate the possible T-cell infiltration into the brain parenchyma to exclude their recruitment in an earlier stage and the consequent possible interaction with the resident immune cells. Despite the absence of a significant blood Tregs participation, we found changes in immune-related gene expression in the hippocampus in response to SNI. Of interest, in the 1-month neuropathic mice, but not in the 12-month neuropathic mice, we detected an enhancement of several genes, most of them involved in inflammation and apoptosis signaling pathways. We found an increased expression of IL-1β together with an upregulation of other substrates, such as Nf-Kb, C3, CD38, CD68, and Socs2, widely recognized as markers of neuroinflammation, brain damage, and aging.[8,31,65] Therefore, we described the dysregulation of a number of immunomodulatory molecules, suggesting a hippocampal neuroinflammatory response, which may contribute to the SNI phenotype. Besides the immunoregulatory activity, IL-1 β can negatively regulate hippocampal synaptic plasticity.[6,41] Thus, we cannot exclude that increase of IL-1β may be, at least partly, responsible for impaired LTP in the 1-month SNI mice by compromising memory and learning processes.[36,53,55]

The huge upregulation of CD38 (15.4-fold), also found in the 12-month sham mice compared with the 1-month sham animals, suggests a possible aging-related accumulation of M1 polarized macrophage and NAD decrease.[22] We found an increased expression of CCR2, the specific CCL2 (MCP-1) chemokine receptor, previously shown to crucially participate in the chronic pain development[1,52] and to colocalize with either dopaminergic or cholinergic neurons in different brain regions where it modulates extravasation and migration of monocytes to the inflammatory sites.[18] The substantial upregulation of macrophage colony-stimulating factor-1 suggests an increased susceptibility of mononuclear phagocytes to ECM proteins' stimulation and their consequent activation, which is associated

with postinjury regeneration rather than with a mere proinflammatory function.[39] Worthy of note was also the relevant increase of transferrin-bound iron uptake, as demonstrated by the huge induction of transferrin receptor TFRC, as a metabolic reorganization after injury. Such substantial modifications were not detectable in the 12-month SNI mice. These findings may be in agreement with the partial restoration of the behavioral (and electrophysiological) phenotype. However, the flattening in the neuroinflammatory mediators in the 12-month SNI mice could also be masked by the increased basal levels of those molecules in the matched-aged sham mice.[7,60] Concerning the PFC, we found that only Tbx21 in the 1-month SNI mice, and Ctla4 and Vcam in the 12-month SNI mice reached the significance, among the nearly 50 deregulated genes. Worth mentioning, a detailed analysis of differential DNA methylation in the PFC of SNI mice, performed by Topham et al.,[63] revealed an interesting time-specific CpG methylation dynamics. Although not including any of the 3 deregulated PFC genes identified in our study, the observed methylation profile could fairly imply a functional outcome similar to the one postulated on the bases of our findings, as denoted by gene ontology analysis. Indeed, throughout the time course, authors observed a specific enrichment in genes implicated in inflammatory and T-cell adaptive immune responses, including Toll receptor signaling pathway, as well as an involvement of a series of adhesion molecules. Overall, these findings suggest a functional connection with the genes discussed in this study.

5. Limits

First, our analysis does not include the 1-year response to SNI by female sex. This remains an important issue, given also the role of immune cells in the sex differences in pain processing.[2,10,17,41] Second, gene expression analyses have been performed on tissue samples derived from whole PFC and hippocampus homogenates instead of specific subregions. Thus, we cannot exclude that some signal differences may be diluted. Third, we suggest the involvement of molecular pathways (Fig. S2, available at http://links.lww.com/PAIN/B547) in the SNI phenotype, but no molecular mechanism has been investigated. We recognize these limitations, and we propose our findings as a first step towards understanding functional changes associated with long-term neuropathic pain.

6. Conclusions

Our data indicate that the 1-year SNI condition is not associated with cognitive impairments, suggesting that distinct brain circuits may drive the psychiatric components of neuropathic pain. Moreover, this study suggests that hippocampal neuroinflammation may influence the development of affective feature of neuropathic pain. This study paves the way for better investigation of the long-term consequences of peripheral nerve injury in which most of the available drugs are to date unsatisfactory.

Conflict of interest statement

The authors have no conflicts of interest to declare.

Acknowledgments

Supported by VALERE research program (2017) from University of Campania "Luigi Vanvitelli" to Francesca Guida.

Appendix A. Supplemental digital content

Supplemental digital content associated with this article can be found online at http://links.lww.com/PAIN/B547.

Article history:
Received 24 September 2021
Received in revised form 4 November 2021
Accepted 18 November 2021
Available online 3 December 2021

References

[1] Abbadie C, Lindia JA, Cumiskey AM, Peterson LB, Mudgett JS, Bayne EK, DeMartino JA, MacIntyre DE, Forrest MJ. Impaired neuropathic pain responses in mice lacking the chemokine receptor CCR2. Proc Natl Acad Sci U S A 2003;100:7947–52.
[2] Alessio N, Belardo C, Trotta MC, Paino S, Boccella S, Gargano F, Pieretti G, Ricciardi F, Marabese I, Luongo L, Galderisi U, D'Amico M, Maione S, Guida F. Vitamin D deficiency induces chronic pain and microglial phenotypic changes in mice. Int J Mol Sci 2021;22:3604.
[3] Apkarian AV, Mutso AA, Centeno MV, Kan L, Wu M, Levinstein M, Banisadr G, Gobeske KT, Miller RJ, Radulovic J, Hen R, Kessler JA. Role of adult hippocampal neurogenesis in persistent pain. PAIN 2016;157:418–28.
[4] Bakker A, Kirwan CB, Miller M, Stark CE. Pattern separation in the human hippocampal CA3 and dentate gyrus. Science 2008;319:1640–2.
[5] Barcelon EE, Cho WH, Jun SB, Lee SJ. Brain microglial activation in chronic pain-associated affective disorder. Front Neurosci 2019;13:213.
[6] Barrientos RM, Higgins EA, Sprunger DB, Watkins LR, Rudy JW, Maier SF. Memory for context is impaired by a post context exposure injection of interleukin-1 beta into dorsal hippocampus. Behav Brain Res 2002;134:291–8.
[7] Barrientos RM, Kitt MM, Watkins LR, Maier SF. Neuroinflammation in the normal aging hippocampus. Neuroscience 2015;309:84–99.
[8] Basrai HS, Turnley AM. The suppressor of cytokine signalling 2 (SOCS2), traumatic brain injury and microglial/macrophage regulation. Neural Regen Res 2016;11:1405–6.
[9] Belardo C, Iannotta M, Boccella S, Rubino RC, Ricciardi F, Infantino R, Pieretti G, Stella L, Paino S, Marabese I, Maisto R, Luongo L, Maione S, Guida F. Oral cannabidiol prevents allodynia and neurological dysfunctions in a mouse model of mild traumatic brain injury. Front Pharmacol 2019;10:352.
[10] Boccella S, Cristiano C, Romano R, Iannotta M, Belardo C, Farina A, Guida F, Piscitelli F, Palazzo E, Mazzitelli M, Imperatore R, Tunisi L, de Novellis V, Cristino L, Di Marzo V, Calignano A, Maione S, Luongo L. Ultramicronized palmitoylethanolamide rescues the cognitive decline-associated loss of neural plasticity in the neuropathic mouse entorhinal cortex-dentate gyrus pathway. Neurobiol Dis 2019;121:106–19.
[11] Boccella S, Guida F, De Logu F, De Gregorio D, Mazzitelli M, Belardo C, Iannotta M, Serra N, Nassini R, de Novellis V, Geppetti P, Maione S, Luongo L. Ketones and pain: unexplored role of hydroxyl carboxylic acid receptor type 2 in the pathophysiology of neuropathic pain. FASEB J 2019;33:1062–73.
[12] Bolz L, Heigele S, Bischofberger J. Running improves pattern separation during novel object recognition. Brain Plast 2015;1:129–41.
[13] Bruel-Jungerman E, Davis S, Rampon C, Laroche S. Long-term potentiation enhances neurogenesis in the adult dentate gyrus. J Neurosci 2006;26:5888–93.
[14] Burke SN, Wallace JL, Hartzell AL, Nematollahi S, Plange K, Barnes CA. Age-associated deficits in pattern separation functions of the perirhinal cortex: a cross-species consensus. Behav Neurosci 2011;125:836–47.
[15] Calvo M, Dawes JM, Bennett DL. The role of the immune system in the generation of neuropathic pain. Lancet Neurol 2012;11:629–42.
[16] Cès A, Burg T, Herbeaux K, Héraud C, Bott JB, Mensah-Nyagan AG, Mathis C. Age-related vulnerability of pattern separation in C57BL/6J mice. Neurobiol Aging 2018;62:120–9.
[17] Chan DV, Gibson HM, Aufiero BM, Wilson AJ, Hafner MS, Mi Q-S, Wong HK. Differential CTLA-4 expression in human CD4+ versus CD8+ T cells is associated with increased NFAT1 and inhibition of CD4+ proliferation. Genes Immun 2014;15:25–32.
[18] Chu HX, Arumugam TV, Gelderblom M, Magnus T, Drummond GR, Sobey CG. Role of CCR2 in inflammatory conditions of the central nervous system. J Cereb Blood Flow Metab 2014;34:1425–9.
[19] Clelland CD, Choi M, Romberg C, Clemenson GD Jr, Fragniere A, Tyers P, Jessberger S, Saksida LM, Barker RA, Gage FH, Bussey TJ. A

functional role for adult hippocampal neurogenesis in spatial pattern separation. Science 2009;325:210–3.
[20] Coraggio V, Guida F, Boccella S, Scafuro M, Paino S, Romano D, Maione S, Luongo L. Neuroimmune-driven neuropathic pain establishment: a focus on gender differences. Int J Mol Sci 2018;19:281.
[21] Costigan M, Moss A, Latremoliere A, Johnston C, Verma-Gandhu M, Herbert TA, Barrett L, Brenner GJ, Vardeh D, Woolf CJ, Fitzgerald M. T-cell infiltration and signaling in the adult dorsal spinal cord is a major contributor to neuropathic pain-like hypersensitivity. J Neurosci 2009;29:14415–22.
[22] Covarrubias AJ, Kale A, Perrone R, Lopez-Dominguez JA, Pisco AO, Kasler HG, Schmidt MS, Heckenbach I, Kwok R, Wiley CD, Wong HS, Gibbs E, Iyer SS, Basisty N, Wu Q, Kim IJ, Silva E, Vitangcol K, Shin KO, Lee YM, Riley R, Ben-Sahra I, Ott M, Schilling B, Scheibye-Knudsen M, Ishihara K, Quake SR, Newman J, Brenner C, Campisi J, Verdin E. Senescent cells promote tissue NAD(+) decline during ageing via the activation of CD38(+) macrophages. Nat Metab 2020;2:1265–83.
[23] Decosterd I, Woolf CJ. Spared nerve injury: an animal model of persistent peripheral neuropathic pain. PAIN 2000;87:149–58.
[24] Deng W, Mayford M, Gage FH. Selection of distinct populations of dentate granule cells in response to inputs as a mechanism for pattern separation in mice. Elife 2013;2:e00312.
[25] Deuis JR, Dvorakova LS, Vetter I. Methods used to evaluate pain behaviors in rodents. Front Mol Neurosci 2017;10:284.
[26] Dick BD, Rashiq S. Disruption of attention and working memory traces in individuals with chronic pain. Anesth Analg 2007;104:1223. tables of contents.
[27] Dimitrov EL, Tsuda MC, Cameron HA, Usdin TB. Anxiety- and depression-like behavior and impaired neurogenesis evoked by peripheral neuropathy persist following resolution of prolonged tactile hypersensitivity. J Neurosci 2014;34:12304–12.
[28] DosSantos MF, Moura BS, DaSilva AF. Reward circuitry plasticity in pain perception and modulation. Front Pharmacol 2017;8:790.
[29] Gattlen C, Clarke CB, Piller N, Kirschmann G, Pertin M, Decosterd I, Gosselin RD, Suter MR. Spinal cord T-cell infiltration in the rat spared nerve injury model: a time course study. Int J Mol Sci 2016;17:352.
[30] Goffer Y, Xu D, Eberle SE, D'Amour J, Lee M, Tukey D, Froemke RC, Ziff EB, Wang J. Calcium-permeable AMPA receptors in the nucleus accumbens regulate depression-like behaviors in the chronic neuropathic pain state. J Neurosci 2013;33:19034–44.
[31] Guerreiro S, Privat AL, Bressac L, Toulorge D. CD38 in neurodegeneration and neuroinflammation. Cells 2020;9:471.
[32] Gui WS, Wei X, Mai CL, Murugan M, Wu LJ, Xin WJ, Zhou LJ, Liu XG. Interleukin-1β overproduction is a common cause for neuropathic pain, memory deficit, and depression following peripheral nerve injury in rodents. Mol Pain 2016;12:1744806916646784.
[33] Guida F, Boccella S, Iannotta M, De Gregorio D, Giordano C, Belardo C, Romano R, Palazzo E, Scafuro MA, Serra N, de Novellis V, Rossi F, Maione S, Luongo L. Palmitoylethanolamide reduces neuropsychiatric behaviors by restoring cortical electrophysiological activity in a mouse model of mild traumatic brain injury. Front Pharmacol 2017;8:95.
[34] Guida F, De Gregorio D, Palazzo E, Ricciardi F, Boccella S, Belardo C, Iannotta M, Infantino R, Formato F, Marabese I, Luongo L, de Novellis V, Maione S. Behavioral, biochemical and electrophysiological changes in spared nerve injury model of neuropathic pain. Int J Mol Sci 2020;21:3396.
[35] Hayakawa K, Esposito E, Wang X, Terasaki Y, Liu Y, Xing C, Ji X, Lo EH. Transfer of mitochondria from astrocytes to neurons after stroke. Nature 2016;535:551–5.
[36] Hoshino K, Hasegawa K, Kamiya H, Morimoto Y. Synapse-specific effects of IL-1β on long-term potentiation in the mouse hippocampus. Biomed Res 2017;38:183–8.
[37] Humo M, Lu H, Yalcin I. The molecular neurobiology of chronic pain-induced depression. Cell Tissue Res 2019;377:21–43.
[38] Ishikawa A, Ambroggi F, Nicola SM, Fields HL. Dorsomedial prefrontal cortex contribution to behavioral and nucleus accumbens neuronal responses to incentive cues. J Neurosci 2008;28:5088–98.
[39] Jones CV, Ricardo SD. Macrophages and CSF-1: implications for development and beyond. Organogenesis 2013;9:249–60.
[40] Kaplan MH. STAT4. Immunol Res 2005;31:231–41.
[41] Khairova RA, Machado-Vieira R, Du J, Manji HK. A potential role for pro-inflammatory cytokines in regulating synaptic plasticity in major depressive disorder. Int J Neuropsychopharmacol 2009;12:561–78.
[42] Laumet G, Ma J, Robison AJ, Kumari S, Heijnen CJ, Kavelaars A. T cells as an emerging target for chronic pain therapy. Front Mol Neurosci 2019;12:216.
[43] Lazarevic V, Glimcher LH, Lord GM. T-bet: a bridge between innate and adaptive immunity. Nat Rev Immunol 2013;13:777–89.
[44] Lazic SE. Modeling hippocampal neurogenesis across the lifespan in seven species. Neurobiol Aging 2012;33:1664–71.
[45] Liu Y, Zhou LJ, Wang J, Li D, Ren WJ, Peng J, Wei X, Xu T, Xin WJ, Pang RP, Li YY, Qin ZH, Murugan M, Mattson MP, Wu LJ, Liu XG. TNF-α differentially regulates synaptic plasticity in the Hippocampus and spinal cord by microglia-dependent mechanisms after peripheral nerve injury. J Neurosci 2017;37:871–81.
[46] Mai L, Zhu X, Huang F, He H, Fan W. p38 mitogen-activated protein kinase and pain. Life Sci 2020;256:117885.
[47] Malcangio M. Role of the immune system in neuropathic pain. Scand J Pain 2019;20:33–7.
[48] Mansour A, Baria AT, Tetreault P, Vachon-Presseau E, Chang PC, Huang L, Apkarian AV, Baliki MN. Global disruption of degree rank order: a hallmark of chronic pain. Sci Rep 2016;6:34853.
[49] Martinez E, Lin HH, Zhou H, Dale J, Liu K, Wang J. Corticostriatal regulation of acute pain. Front Cel Neurosci 2017;11:146.
[50] Maurer AP, Johnson SA, Hernandez AR, Reasor J, Cossio DM, Fertal KE, Mizell JM, Lubke KN, Clark BJ, Burke SN. Age-related changes in lateral entorhinal and CA3 neuron allocation predict poor performance on object discrimination. Front Syst Neurosci 2017;11:49.
[51] Metz AE, Yau HJ, Centeno MV, Apkarian AV, Martina M. Morphological and functional reorganization of rat medial prefrontal cortex in neuropathic pain. Proc Natl Acad Sci U S A 2009;106:2423–8.
[52] Miller RE, Tran PB, Das R, Ghoreishi-Haack N, Ren D, Miller RJ, Malfait AM. CCR2 chemokine receptor signaling mediates pain in experimental osteoarthritis. Proc Natl Acad Sci U S A 2012;109:20602–7.
[53] Murray CA, Lynch MA. Evidence that increased hippocampal expression of the cytokine interleukin-1β is a common trigger for age-and stress-induced impairments in long-term potentiation. J Neurosci 1998;18:2974–81.
[54] Neugebauer V, Galhardo V, Maione S, Mackey SC. Forebrain pain mechanisms. Brain Res Rev 2009;60:226–42.
[55] O'Connor JJ, Coogan AN. Actions of the pro-inflammatory cytokine Il-1 [beta] on central synaptic transmission. Exp Physiol 1999;84:601–14.
[56] Palazzo E, Luongo L, Guida F, Marabese I, Romano R, Iannotta M, Rossi F, D'Aniello A, Stella L, Marmo F, Usiello A, de Bartolomeis A, Maione S, de Novellis V. D-Aspartate drinking solution alleviates pain and cognitive impairment in neuropathic mice. Amino Acids 2016;48:1553–67.
[57] Roth LR, Leung LS. Difference in LTP at basal and apical dendrites of CA1 pyramidal neurons in urethane-anesthetized rats. Brain Res 1995;694:40–8.
[58] Sellmeijer J, Mathis V, Hugel S, Li XH, Song Q, Chen QY, Barthas F, Lutz PE, Karatas M, Luthi A, Veinante P, Aertsen A, Barrot M, Zhuo M, Yalcin I. Hyperactivity of anterior cingulate cortex areas 24a/24b drives chronic pain-induced anxiodepressive-like consequences. J Neurosci 2018;38:3102–15.
[59] Shen H, Kalivas PW. Reduced LTP and LTD in prefrontal cortex synapses in the nucleus accumbens after heroin self-administration. Int J Neuropsychopharmacol 2013;16:1165–7.
[60] Sparkman NL, Johnson RW. Neuroinflammation associated with aging sensitizes the brain to the effects of infection or stress. Neuroimmunomodulation 2008;15:323–30.
[61] Su C, Lin HY, Yang R, Xu D, Lee M, Pawlak N, Norcini M, Sideris A, Recio-Pinto E, Huang D, Wang J. AMPAkines target the nucleus accumbens to relieve postoperative pain. Anesthesiology 2016;125:1030–43.
[62] ten Dijke P, Hill CS. New insights into TGF-beta-Smad signalling. Trends Biochem Sci 2004;29:265–73.
[63] Topham L, Gregoire S, Kang H, Salmon-Divon M, Lax E, Millecamps M, Szyf M, Stone LS. The transition from acute to chronic pain: dynamic epigenetic reprogramming of the mouse prefrontal cortex up to 1 year after nerve injury. PAIN 2020;161:2394–409.
[64] van Hagen BT, van Goethem NP, Lagatta DC, Prickaerts J. The object pattern separation (OPS) task: a behavioral paradigm derived from the object recognition task. Behav Brain Res 2015;285:44–52.
[65] Waller R, Baxter L, Fillingham DJ, Coelho S, Pozo JM, Mozumder M, Frangi AF, Ince PG, Simpson JE, Highley JR. Iba-1-/CD68+ microglia are a prominent feature of age-associated deep subcortical white matter lesions. PLoS One 2019;14:e0210888.
[66] Wang VC, Mullally WJ. Pain neurology. Am J Med 2020;133:273–80.
[67] Yalcin I, Aksu F, Belzung C. Effects of desipramine and tramadol in a chronic mild stress model in mice are altered by yohimbine but not by pindolol. Eur J Pharmacol 2005;514:165–74.
[68] Zhou H, Martinez E, Lin HH, Yang R, Dale JA, Liu K, Huang D, Wang J. Inhibition of the prefrontal projection to the nucleus accumbens enhances pain sensitivity and affect. Front Cel Neurosci 2018;12:240.